Published in final edited form as:
Mol Cell. 2009 October 23; 36(2): 207–218. doi:10.1016/j.molcel.2009.09.017.

Conserved Telomere maintenance Component 1 interacts with STN1 and maintains chromosome ends in higher eukaryotes

Yulia V. Surovtseva[1,3], **Dmitri Churikov**[2], **Kara A. Boltz**[1], **Xiangyu Song**[1], **Jonathan C. Lamb**[1], **Ross Warrington**[1,4], **Katherine Leehy**[1], **Michelle Heacock**[1,5], **Carolyn M. Price**[2,6], and **Dorothy E. Shippen**[1,6]

[1]Department of Biochemistry and Biophysics, Texas A&M University, 2128 TAMU, College Station, Texas 77843-2128, USA

[2]Department of Cancer and Cell Biology, University of Cincinnati, Cincinnati, Ohio 45267, USA

Summary

Orthologs of the yeast telomere protein Stn1 are present in plants, but other components of the Cdc13/Stn1/Ten1 (CST) complex have only been found in fungi. Here we report the identification of Conserved Telomere maintenance Component 1 (CTC1) in plants and vertebrates. CTC1 encodes an ~140 kDa telomere-associated protein predicted to contain multiple OB-fold domains. *Arabidopsis* mutants null for *CTC1* display a severe telomere deprotection phenotype accompanied by a rapid onset of developmental defects and sterility. Telomeric and subtelomeric tracts are dramatically eroded, and chromosome ends exhibit increased G-overhangs, recombination, and end-to-end fusions. AtCTC1 both physically and genetically interacts with AtSTN1. Depletion of human CTC1 by RNAi triggers a DNA damage response, chromatin bridges, increased G-overhangs and sporadic telomere loss. These data indicate that CTC1 participates in telomere maintenance in diverse species and that a CST-like complex is required for telomere integrity in multicellular organisms.

Introduction

The terminus of a linear chromosome must be distinguished from a double-strand break to avoid deleterious nucleolytic attack and recruitment into DNA repair reactions. Telomeres prevent such actions by forming a protective cap on the chromosome end. This cap consists of an elaborate, higher-order DNA architecture and a suite of telomere-specific proteins. The formation of a t-loop of telomeric DNA is thought to play an important role in sequestering the terminal single-strand G-overhang from harmful activities (de Lange, 2004; Wei and Price, 2003), while double-strand (ds) and single-strand (ss) telomeric DNA binding proteins coat the chromosome terminus to further distinguish it from a double-strand break (Palm and de Lange, 2008)

6Corresponding Authors: Dorothy Shippen, Department of Biochemistry and Biophysics, Texas A&M University, 2128 TAMU, College Station, TX 77843-2128, Carolyn Price, Department of Cancer and Cell Biology, University of Cincinnati, 3125 Eden Avenue, Cincinnati, Ohio 45267-0521.
[3]Current addresses: Department of Pathology, Yale University School of Medicine, P.O. Box 208023, New Haven, CT 06520-8023, USA.
[4]Current addresses: Department of Pharmacology, Howard Hughes Medical Institute, University of Texas Southwestern Medical Center Dallas, Texas 75390.
[5]Current addresses: Laboratory of Structural Biology, National Institute of Environmental Health Sciences, National Institutes of Health, Research Triangle Park, NC 27709, USA.

In *Saccharomyces cerevisiae*, telomeres are bound by a trimeric protein complex, termed CST, composed of Cdc13, Stn1 and Ten1 (Gao et al., 2007; Lundblad, 2006). The three proteins interact to form an RPA-like complex with specificity for ss telomeric DNA. Cdc13 and Stn1 harbor at least one oligonucleotide-oligosaccharide binding (OB) fold, which in the case of Cdc13 is exploited to bind to the G-overhang (Guo et al., 2007; Mitton-Fry et al., 2002). Stn1 and Ten1 associate with the overhang primarily via interactions with Cdc13. The CST complex plays a key role in telomere length regulation (Bianchi and Shore, 2008). Cdc13 recruits the telomerase RNP via a direct interaction with the Est1 component of telomerase (Bianchi et al., 2004; Chandra et al., 2001), while Stn1 is thought to inhibit telomerase action by competing with Est1 for Cdc13 binding (Li et al., 2009; Puglisi et al., 2008). In addition, Cdc13 and Stn1 contribute to coupling of G- and C-strand synthesis through interactions with DNA polymerase α (Grossi et al., 2004; Qi and Zakian, 2000).

The CST complex is also essential for chromosome end-protection. Mutations in any one of the CST components result in degradation of the C-strand, accumulation of ss G-rich telomeric DNA and late S/G2 cell cycle arrest (Garvik et al., 1995; Grandin et al., 2001; Grandin et al., 1997). Telomere protection appears to be facilitated primarily by Stn1 and Ten1, and overexpression of Stn1 and Ten1 can rescue the lethality of Cdc13 depletion (Grandin et al., 2001; Petreaca et al., 2007; Puglisi et al., 2008). Finally, Cdc13 and Stn1 also inhibit telomere recombination (Iyer et al., 2005; Petreaca et al., 2006; Zubko and Lydall, 2006).

Mammalian telomeres are bound by shelterin, a six-member complex that, unlike CST, binds both ss and ds telomeric DNA (Palm and de Lange, 2008). The shelterin proteins TRF1 and TRF2 coat ds telomeric DNA, while POT1 binds the ss G-overhang. The TRF1/TRF2-interacting protein TIN2 and the POT1-interacting protein TPP1 associate with each other, providing a bridge between the duplex and ss regions of telomeric DNA. RAP1 associates with telomeres via interaction with TRF2. The majority of shelterin components are implicated in telomere capping, although TRF2 and POT1 appear to play pivotal roles in this process. TRF2 associates with telomeric DNA via a myb-like DNA binding domain. Loss of telomere-bound TRF2 results in immediate degradation of the G-overhang and end-to-end chromosome fusions (Celli and de Lange, 2005), while certain dominant negative alleles cause rapid telomere shortening with extrusion of extra-chromosomal telomeric circles via homologous recombination (Wang et al., 2004).

Like components of the CST complex, POT1 and its partner TPP1 harbor OB-folds. POT1 binds directly to the overhang through two adjacent OB-folds, thus sequestering the DNA 3′ terminus and reducing access to telomerase (Lei et al., 2004; Lei et al., 2005). TPP1 does not bind DNA directly, but dimerization with POT1 increases the DNA-binding affinity of POT1 by ~10 fold (Wang et al., 2007). Knockdown of human POT1 by RNAi causes a fairly mild phenotype characterized by impaired proliferation, an increase in chromosome fusions, decreased G-overhang signals and an increase in telomere length (Hockemeyer et al., 2005; Veldman et al., 2004; Yang et al., 2005; Ye et al., 2004). Disruption of the *POT1* gene leads to more dire consequences (Churikov et al., 2006; Hockemeyer et al., 2006; Wu et al., 2006) including activation of a strong ATR-mediated DNA damage checkpoint, G-overhang elongation, rapid telomere growth, elevated telomere recombination and ultimately cell death (Churikov and Price, 2008; Denchi and de Lange, 2007; Guo et al., 2007).

Telomere protein composition may be more conserved than previously surmised (Linger and Price, 2009). At least one shelterin component, Rap1, is present in *S. cerevisiae*, although unlike vertebrate RAP1, ScRap1p directly binds ds telomeric DNA through two myb-like DNA binding domains and contributes to telomere length regulation and telomere silencing (Lundblad, 2006). Likewise, fission yeast contain several shelterin orthologs including Taz1, an ortholog of mammalian TRF1/TRF2 proteins (Cooper et al., 1997), and Pot1 (Baumann and

Cech, 2001). Furthermore, recent purification of SpPot1-associated proteins identified Tpz1, a presumed ortholog of vertebrate TPP1 (Miyoshi et al., 2008). Like TPP1, Tpz1 contains an OB-fold, and physical association of SpPot1 and Tpz1 is required for chromosome end protection (Miyoshi et al., 2008; Xin et al., 2007). The Pot1-Tpz1 complex recruits two additional proteins, Ccq1 and Poz1. Poz1 serves as a bridge linking the Pot1-Tpz1 complex to the ds telomere proteins Rap1 and Taz1 in a manner similar to the shelterin component TIN2 (Miyoshi et al., 2008). Altogether, these findings argue that the core components of the shelterin complex are evolutionary conserved.

Emerging data indicate that CST components are also widespread. Although Cdc13 orthologs have yet to be uncovered outside of *S. cerevisiae*, a Stn1/Ten1 capping complex was recently described for *S. pombe* (Martin et al., 2007). Both proteins localize to telomeres and are essential for chromosome end protection from exonucleases and telomere fusions. Notably, no direct physical association between Stn1/Ten1 and Pot1 has been observed (Martin et al., 2007) and mass spectrometry of SpPot1-associated factors failed to identify Stn1 or Ten1 (Miyoshi et al., 2008). These findings suggest that CST and shelterin components may constitute distinct telomere complexes.

Plants also appear to harbor both shelterin and CST components. Several Myb-containing TRF-like proteins from *Arabidopsis* bind telomeric dsDNA in vitro (Zellinger and Riha, 2007) and in rice genetic data implicate one of these, RTBP1, in chromosome end protection (Hong et al., 2007). *Arabidopsis* encodes three OB-fold bearing POT1-like proteins (Shakirov et al., 2005; Surovtseva et al., 2007)(A. Nelson, Y. Surovtseva and D. Shippen, unpublished data). Interestingly, while over-expression of a dominant negative allele of AtPOT1b or depletion of AtPOT1c lead to a telomere uncapping phenotype similar to a *pot1* deficiency in yeast and mammals (Shakirov et al., 2005)(A. Nelson, Y. Surovtseva and D. Shippen, unpublished data), AtPOT1a is dispensable for chromosome end protection and instead is required for telomerase function (Surovtseva et al., 2007). Currently, orthologs for TIN2, RAP1 and TPP1 cannot be discerned in any plant genome.

Recently, a distant homolog of the CST component STN1 was uncovered in *Arabidopsis* (Song et al., 2008). AtSTN1 bears a single OB-fold and localizes to telomeres in vivo. Deletion of AtSTN1 results in the rapid onset of growth defects and sterility, coupled with extensive exonucleolytic degradation of chromosome ends, increased telomere recombination, and massive end-to-end chromosome fusion (Song et al., 2008).

Here we report the identification of a new telomere protein, termed CTC1 (Conserved Telomere maintenance Component 1), that physically and genetically interacts with AtSTN1. We show that AtCTC1 localizes to telomeres in vivo and, as for AtSTN1, loss of AtCTC1 triggers rapid telomere deprotection resulting in gross developmental and morphological defects, abrupt telomere loss, telomere recombination and genome instability. Although not as severe as an *Arabidopsis ctc1* null mutant, the consequences of CTC1 knockdown in human cells include a DNA damage response, formation of chromatin bridges, increased G-overhang signals and loss of telomeric DNA from some chromosome ends. Altogether, these data argue that CTC1 is a component of a CST-like complex in multicellular organisms that is needed for telomere integrity. Notably, we found that mammalian CTC1 and STN1 correspond to the two subunits of alpha accessory factor (AAF), a protein complex previously shown to stimulate mammalian DNA pol α-primase (Casteel et al., 2009; Goulian and Heard, 1990). Thus, the CST-like complex from plants and mammals may resemble the *S. cerevisiae* CST by providing a link between telomeric G- and C-strand synthesis.

Results

Identification of CTC1

In an effort to identify mutations in *AtPOT1c*, we examined lines within a TILLING collection of EMS-mutagenized *Arabidopsis* plants. A mutant was uncovered that showed a profound telomere uncapping phenotype (described below). However, this phenotype did not segregate with nucleotide changes in *AtPOT1c* and therefore map-based cloning was employed to identify the lesion responsible for the phenotype. A single-nucleotide transition (G to A) was found in At4g09680, which co-segregated with telomere uncapping. At4g09680 lies on chromosome 4, while *AtPOT1c* resides on chromosome 2. At4g09680 was designated *CTC1* (Conserved Telomere maintenance Component 1) and the point mutant was termed *ctc1-1*. *CTC1* is a single copy gene and sequence analysis of *CTC1* cDNA from wild type plants revealed a large ORF with 16 exons that encodes a previously uncharacterized 142 kDa protein (Figure 1A). RT-PCR demonstrated that *CTC1* is widely expressed in both vegetative and reproductive organs (Figure S1A). Further analysis of the CTC1 protein sequence is discussed below.

CTC1 associates with telomeres in vivo

To determine whether CTC1 associates with telomeres in vivo, an N-terminal CFP-tagged version of CTC1 protein was expressed in transgenic *Arabidopsis* and immunolocalization experiments were performed on different tissues. Nuclear CFP signal was detected in plants expressing CFP-CTC1, but not in untransformed controls (Figure 1B, Figure S1B and data not shown). Telomere distribution was analyzed by fluorescence in-situ hybridization (FISH) using a telomere probe. In *Arabidopsis*, telomeres lie at the nucleolar periphery (Armstrong et al., 2001) (Song et al., 2008) and, as expected, telomeric FISH signals were positioned in this location. Similarly, CFP-CTC1 was distributed in a punctate pattern surrounding the nucleolus. A merge of these images showed that much of the CFP-CTC1 co-localized with *Arabidopsis* telomeres (Figure 1B and Figure S1B). CTC1 association with telomeres was quantitated in flowers and seedlings, which contain cycling cells. On average, 51% (n=38, SD=+/-26%) of the telomere signals overlapped with CFP-CTC1. To determine if CTC1 co-localization with telomeres was retained in non-cycling cells, we examined the apical half of rosette leaves that were at least two weeks old and arrested in G1 (Donnelly et al, 1999). In these cells, 44.1% (n=28, standard deviation=+/-24.5%) of the telomeres displayed an overlapping signal with CFP-CTC1. These data argue that CTC1 associates with telomeres throughout the cell cycle.

Severe growth defects and sterility in first generation ctc1 mutants

We next examined the impact of CTC1 inactivation on plant morphology. Sequence analysis of *CTC1* cDNA from *ctc1-1* mutants revealed that the G(1935)A point mutation resulted in a nonsense codon within the ninth exon (Figure 1A). Two additional *CTC1* alleles, *ctc1-2* and *ctc1-3*, bearing T-DNA insertions in the sixth exon or tenth intron, respectively, were identified within the SALK database (Figure 1A). RT-PCR analysis showed that no *CTC1* full length mRNA was produced in either *ctc1-2* or *ctc1-3*, indicating that these lines are null alleles of *AtCTC1* (Figure S1C).

All three *ctc1* mutants displayed a rapid onset of severe morphological defects in the first generation (Figure 1C), confirming that *CTC1* lesions are responsible for telomere uncapping. The large majority of *ctc1* plants had grossly distorted floral phyllotaxy with an irregular branching pattern and fasciated (thick and broad) main and lateral stems and siliques (Figure 1C). Although most mutants produced an influorescence bolt, this structure was highly variable in size, ranging from very short to wild type (Figure 1C, compare middle and bottom right panels). Flowers and siliques were often fused, and seed yield was typically reduced to ~10%

of wild type. The germination efficiency of the few seeds that could be recovered was extremely low, making propagation to the next generation almost impossible.

Telomere shortening and increased length heterogeneity in ctc1 mutants

Terminal restriction fragment (TRF) analysis was performed to examine bulk telomere length in *ctc1* plants derived from a single self-pollinated heterozygous parent. In contrast to the telomeres of their wild type and heterozygous siblings, which spanned 2-5 kb in length (Figure 2A, lanes 1 to 4), telomeres in homozygous *ctc1-1* mutants were severely deregulated (Figure 2A, lanes 5 and 6). The longest *ctc1-1* telomeres were in the wild type range, but a new population of shorter telomeres emerged, the shortest of which trailed to 0.5 kb. Homozygous *ctc1-2* and *ctc1-3* mutants showed a similar aberrant telomere length phenotype (Figure S2A).

We investigated how individual telomeres were affected by CTC1 loss using subtelomeric TRF analysis with probes directed at specific chromosome termini. As expected (Shakirov and Shippen, 2004), sharp bands were produced from wild type telomeres (Figures 2B and S2B). In contrast, telomeres in *ctc1* mutants gave rise to a broad heterogeneous hybridization signal spanning 1.5 kb (Figures 2B and S2B). Primer extension telomere repeat amplification (PETRA) also generated broad smears in *ctc1* mutants (Figure 2C), confirming that the length of individual telomere tracts was grossly deregulated. Telomere shortening and increased heterogeneity at individual telomere tracts in *ctc1* mutants is not due to a reduction in telomerase activity. Quantitative telomere repeat amplification (Q-TRAP) revealed no significant difference in the in vitro telomerase activity levels in *ctc1* mutants relative to wild type (Figure S3).

Increased G-overhang signals and telomere recombination in ctc1 mutants

Next we studied the G-overhang status in *ctc1* mutants using non-denaturing in-gel hybridization. Strikingly, the G-overhang signal was ~three times greater in *ctc1* mutants relative to wild type (3.5±0.7) (Figure 2D). A similar increase in G-overhang signal is observed in *Arabidopsis stn1* mutants (Song et al. 2008). Exonuclease treatment reduced the G-overhang signal in *ctc1* mutants by approximately 95%, indicating that the majority of ss telomeric DNA is associated with the chromosome terminus (Figure 2D, left panel).

To investigate whether telomeres in *ctc1* mutants are subjected to increased recombination, we used t-circle amplification (TCA) (Zellinger et al., 2007) to look for evidence of extra-chromosomal telomeric circles (ECTC), a by-product of t-loop resolution. In this procedure, telomere sequences are amplified by phi29, a polymerase with strand displacement activity that generates high molecular weight ssDNA products from a circular template. As a positive control, TCA was performed on DNA from *ku70* mutants previously shown to accumulate ECTCs (Zellinger et al., 2007). A high molecular weight DNA band was detected in both *ku70* and *ctc1* DNA samples, but not in wild type (Figure 3A). To verify the presence of ECTCs in *ctc1* mutants, we employed the bubble trapping technique (Mesner et al., 2006), which relies on the ability of linear DNA fragments to enter the gel, while circular DNA cannot. A telomeric signal was detected in the well with DNA from *ctc1* and *ku70* mutants, but not with wild type (Figure 3B). These data confirm that ECTCs accumulate in the *ctc1* background and argue that loss of CTC1 results in elevated rates of homologous recombination at telomeres. Altogether, these results indicate that the architecture of the chromosome terminus is perturbed in the absence of CTC1.

End-to-end chromosome fussions in ctc1 mutants

In *Arabidopsis*, telomeres shorter than 1 kb are prone to end-to-end chromosome fusions (Heacock et al., 2007). Since a substantial fraction of *ctc1* telomeres dropped below this critical threshold, we looked for evidence of mitotic abnormalities. Anaphase bridges were scored in

four individual *ctc1-1* mutants and in their wild type siblings. As expected, there was no evidence of genome instability in wild type plants, but in all four *ctc1-1* mutants a high fraction of mitotic cells (up to 39%) exhibited anaphase bridges (Figure 3C and Table S1). Many anaphases contained multiple bridged chromosomes as well as instances of unequal chromosome segregation (Figure 3C). FISH using a mixture of probes from nine subtelomeric regions produced signals in 20/23 anaphase bridges, indicating that the bridges represent end-to-end fusions (Table 1). FISH probes from eight chromosome ends were individually applied to chromosome preparations from a single *ctc1-1* flower cluster. Signals from each probe were observed in anaphase bridges suggesting that all chromosome arms participated in chromosome fusions (Table 1).

Telomere fusion PCR confirmed end-to-end chromosome fusion. Abundant telomere fusion products were generated from *ctc1-1* homozygous plants, but not from heterozygous or wild type siblings (Figure 3D and data not shown). Sequence analysis of 27 cloned fusion junctions failed to detect joining events involving direct fusion of telomere repeats. Instead, telomere-subtelomere fusions (14%) and subtelomere-subtelomere fusions (86%) were recovered (Figure 3D), which were characterized by extensive loss of subtelomere sequences (792 bp average loss). In contrast, in G9 *tert* mutants, telomere-subtelomere fusions are the most prevalent (78%), and the average loss of subtelomeric DNA sequences is only 290 bp (Heacock et al., 2004). Thus, chromosome ends are subjected to dramatic DNA loss prior to fusion in *ctc1* mutants.

CTC1 and STN1 act in the same genetic pathway for chromosome end protection

Since the rapid telomere uncapping phenotype associated with loss of AtCTC1 is remarkably similar to AtSTN1 deficiency (Song et al., 2008), we asked whether the two proteins act in the same genetic pathway for chromosome end protection. Plants heterozygous for *ctc1-1* were crossed to *stn1-1* heterozygotes and F1 progeny were self-pollinated to generate homozygous *ctc1-1 stn1-1* mutants, and their *ctc1-1* and *stn1-1* single mutant siblings. The *ctc1 stn1* double mutants were viable, and the severity of morphological defects was similar to the single mutants (Figure S4A). TRF analysis and PETRA revealed the same heterogeneous, shortened telomere profile in double mutants as in the single mutants (Figures 4A and S4B). Similarly, G-overhang signal intensity and the level of ECTC were comparable, implying that *ctc1-1 stn1-1* double mutants did not undergo additional telomeric DNA depletion or increased telomere recombination (Figures 4B and S4C). Finally, the frequency of anaphase bridges was similar in double mutants and their *ctc1* and *stn1* siblings (Table S2). Altogether these findings indicate that *AtCTC1* and *AtSTN1* act in the same pathway for chromosome end protection.

We looked for evidence of a physical association between AtCTC1 and AtSTN1 proteins. Full length AtSTN1 and truncation fragments of AtCTC1 were expressed in rabbit reticulocyte lysate as T7-tagged proteins or radiolabeled with ^{35}S methionine. Immunoprecipitation experiments showed no interaction between AtSTN1 and fragments A-CTC1 or D-CTC1. However, AtSTN1 bound the B-CTC1 and C-CTC1 fragments in reciprocal immunoprecipitation assays (Figure 4C). The STN1/C-CTC1 interaction was confirmed in a yeast two hybrid assay (data not shown). These data indicate that AtSTN1 and AtCTC1 directly interact in vitro and hence may also associate with each other in vivo.

Genome instability in human cells depleted of CTC1

TBLASTN and EST database searches revealed CTC1 homologs in a wide range of plant species, and searches using PSI-BLAST and HHpred uncovered putative CTC1 orthologs in many vertebrates (see supplemental material for details). Although the putative plant and animal orthologs exhibited considerable sequence divergence, a global profile-profile alignment indicated that the secondary structures had similarity throughout the length of the

protein. Further analysis indicated that the C-terminal domain of human and *Arabidopsis* CTC1 shows homology to OB-fold regions from RPA orthologs, while the N-terminal domain may contain an OB-fold that is distantly related to OB2 from human POT1 (Figures 5A and S5).

Interestingly, the mammalian ortholog of CTC1 is identical to one subunit of Alpha Accessory Factor (AAF-132), while the second subunit of AAF (AAF-44, also known as OBFC1) corresponds to the mammalian ortholog of Stn1 (Casteel et al., 2009; Martin et al., 2007). AAF is a heterodimeric protein that was originally identified as a factor that stimulates Pol α-primase. It was subsequently shown to enhance Pol α-primase association with ssDNA, allowing the enzyme to prime and extend DNA in a reiterative fashion without falling off the DNA template (Goulian and Heard, 1990). Genes encoding the two subunits of AAF were identified recently and AAF-44 was predicted to contain OB-folds resembling those from RPA32 (Casteel et al., 2009).

To investigate whether the human CTC1 protein is important for telomere integrity, we examined the effect of knocking down CTC1 expression in human cells. HeLa and MCF7 cells were subject to two rounds of transfection with individual siRNAs and the level of CTC1 transcript was analyzed by quantitative real-time RT-PCR. Out of eight siRNAs tested, six routinely gave a 60-80% knockdown (Figures 5B and 6C, data not shown). The effect of CTC1 knockdown was monitored after the cells had recovered from the dual transfection.

FACS analysis of DNA content revealed that CTC1 knockdown affected cell cycle progression in MCF7 cells, with cultures showing an accumulation of cells in G1 and a decrease in the S/G2 fraction (Figure S6A). Microscopy of DAPI stained cells revealed that CTC1 knockdown perturbed chromosome segregation. For HeLa cells, we observed an ~2-fold increase in the frequency with which interphase cells remained connected by chromatin bridges (Figures 5C, 5D and S6B). Although the incidence of chromatin bridges was lower in MCF7 cells, there was an increase in the number of cells with micronuclei (Figure S6C). These micronuclei probably reflect anaphase or interphase bridges that were later resolved (Hoffelder et al., 2004). We were unable to determine whether CTC1 knockdown caused an increase in anaphase bridges as the frequency of mitotic cells was too low. However, the cut-like phenotype with interphase bridges is similar to what was observed after POT1 knockdown in HeLa cells (Veldman et al., 2004), suggesting that like *Arabidopsis* CTC1, human CTC1 is needed to prevent chromosome fusions.

To determine whether the defects in chromosome segregation led to a DNA damage response, we looked for the appearance of γH2AX foci. Treatment with CTC1 siRNA caused an increase in foci in both HeLa and MCF7 cells. These foci were fewer in number and larger than the foci observed after UV irradiation. Moreover, they persisted for the duration of the knockdown whereas UV-induced foci were resolved after a few hours (data not shown). We looked for co-localization of γH2AX and TRF2 staining but this was not readily apparent (data not shown) suggesting that either the DNA damage was not telomeric or that disruption of CTC1 results in complete loss of the telomeric tract from a subset of telomeres. Overall, our results indicate that loss of human CTC1 causes a DNA damage response and genome instability.

Depletion of human CTC1 alters G-overhang structure and results in the accumulation of signal-free ends

To determine whether CTC1 knockdown has a direct effect on telomere structure, we used non-denaturing in-gel hybridization to examine the status of the G-overhang. CTC1 depletion caused a modest but consistent increase in ss G-strand DNA in both HeLa and MCF7 cells (Figure 6 and data not shown). In MCF7 cells, the G-strand signal increased by 33 to 41% relative to the non-silencing control siRNA (Figure 6). This increase was statistically significant. Treatment with Exonuclease I removed essentially all the G-strand signal from the

control DNAs, but a small amount remained in the samples from CTC1 depleted cells (Fig. 6A). Thus, removal of CTC1 causes an increase in G-overhang length and may also result in internal regions of ssG-strand DNA.

Given the failure of the γH2AX foci to co-localize with TRF2 after CTC1 knockdown, we analyzed metaphase spreads to determine whether depletion of CTC1 lead to sporadic telomere loss. Metaphase spreads were prepared from siRNA-treated HeLa and 293T cells and hybridized with Cy3-labeled $(TTAGGG)_3$ PNA probe. Subsequent analysis of individual chromosomes revealed an increase in signal free ends (Figure 5 E and F). This increase was statistically significant in 4 out of 6 trials, with the greatest frequency of signal free ends correlating with the deepest CTC1 knockdown (Figure S6D). We therefore conclude that like *Arabidopsis* CTC1, human CTC1 is required to maintain telomere integrity.

Discussion

Although overall telomere architecture and the general mechanism of telomere replication are well conserved, telomere protein sequence and composition have evolved rapidly (Bianchi and Shore, 2008; Linger and Price, 2009). The resulting divergence has complicated telomere protein identification and it is currently unknown whether the full complement of dedicated telomere proteins has been established for any organism. It is also unclear whether additional telomere-specific factors are required to address the unique problems associated with replicating the DNA terminus. In this study we used a forward genetic approach to identify CTC1, a new telomere protein that is required for genome integrity in higher eukaryotes. The *CTC1* gene is predicted to encode a large protein (142 kDa in *Arabidopsis* and 134.5 kDa in humans) that has orthologs dispersed widely throughout the plant and animal kingdoms. Both *Arabidopsis* and human CTC1 interact with STN1, an ortholog of *S. cerevisiae* Stn1 that was recently found at *Arabidopsis* and human telomeres (this study and (Casteel et al., 2009; Dejardin and Kingston, 2009; Song et al., 2008)). Moreover, we discovered that the mammalian CTC1/STN1 complex corresponds to the recently identified DNA polymerase Alpha Accessory Factor (AAF), previously shown to stimulate Pol α-primase (Casteel et al., 2009). Thus, CTC1 appears to be a specialized replication factor that is required for telomere protection and/or telomere replication.

In *Arabidopsis*, the phenotype of a *ctc1* null mutant reflects rapid and catastrophic deprotection of all chromosome ends. Telomere tracts are grossly deregulated in both length and terminal architecture and are subjected to increased recombination and extensive loss of both telomeric and subtelomeric sequences prior to end-to-end fusion. The dramatic effect of CTC1 depletion contrasts with the gradual loss of telomeric DNA in *tert* mutants and the correspondingly later onset of developmental defects (Fitzgerald et al., 1999; Riha et al., 2001). It is striking that plants null for CTC1 are viable because in other model organisms loss of telomere capping proteins activates an ATM or ATR-mediated DNA damage checkpoint and is a lethal event (e.g. loss of *CDC13*, *STN1* or *TEN1* in budding yeast, *STN1*, *TEN1* or *POT1* in fission yeast, and *TRF2* or *POT1* in vertebrates (Churikov and Price, 2008; Grandin et al., 1997; Palm and de Lange, 2008). The extraordinary tolerance of plants to telomere uncapping may reflect a difference in pathways used to monitor genome integrity (Gutierrez, 2005) or the partial duplication of the *Arabidopsis* genome which permits some degree of aneuploidy. In addition, developmental plasticity may mitigate the consequences of genome instability by allowing healthy cells to assume the functions of their more severely compromised neighbors.

Depletion of the human CTC1 mRNA revealed a more modest, but significant role for this protein in promoting telomere integrity. Several cell lines exhibited hallmarks of genome instability such as chromatin bridges, micronuclei and γH2AX staining. Moreover, telomere architecture was perturbed with cells showing an increase in G-overhang signal and sporadic

telomere loss. The milder phenotypes associated with HsCTC1 depletion relative to *Arabidopsis* may reflect the partial knockdown. Plants that are heterozygous for *CTC1* show no deleterious phenotypes, thus only low levels of protein may be needed to maintain telomere integrity. This is the case for vertebrate POT1 as the knockdown causes a less severe phenotype than the full gene knockout (Churikov et al., 2006). It is also possible that the function of HsCTC1 only partially overlaps that of AtCTC1. In *Arabidopsis*, POT1 variants seem to be telomerase subunits rather than stable components of the telomere (C. Cifuentes-Rojas et al. in preparation)(Surovtseva et al., 2007). Thus, plant CTC1 may have evolved to function both in chromosome end protection and telomere replication. In contrast, mammalian CTC1 may function only in telomere replication.

How CTC1 promotes telomere integrity in higher eukaryotes is unknown, but important clues come from recent studies of AAF (HsCTC1/STN1) (Casteel et al). AAF-44 (HsSTN1) contains an OB-fold that is required for AAF to bind ssDNA and stimulate Pol α-primase activity. Thus, as in the budding yeast Cdc13/Stn1/Ten1 (CST) complex, the mammalian CTC1/STN1 complex binds ssDNA and provides a link to the lagging strand replication machinery. This connection also appears to be conserved in plants as AtCTC1 physically interacts with both AtSTN1 (this study) and the DNA pol α catalytic subunit (X. Song and D. Shippen, unpublished data). These findings raise the intriguing possibility that plant and mammalian CTC1 and STN1 are part of a CST complex that, like budding yeast CST, functions in telomere capping and/or coordination of G- and C-strand synthesis during telomere replication. If CTC1 functions in a CST-like complex we would expect higher eukaryotes to possess a Ten1-like protein. Indeed, a putative TEN1 ortholog has been identified in humans (F. Ishikawa, personal communication) and *Arabidopsis* (X. Song, K. Leehy and D. Shippen, unpublished data). Like its counterpart in budding yeast, the *Arabidopsis* TEN1 protein exhibits strong affinity for AtSTN1 in vitro.

The observation that both *S. cerevisiae* CST and mammalian CTC1/STN1 (AAF) modulate DNA pol α-primase is particularly striking. In yeast, both Cdc13 and Stn1 interact with Pol α subunits and are proposed to couple telomeric G- and C-strand synthesis (Grossi et al., 2004; Puglisi et al., 2008; Qi and Zakian, 2000). This coupling prevents accumulation of long G-strand overhangs following G-strand extension by telomerase or C-strand resection by nuclease. Previous studies of mammalian CTC1/STN1 (AAF) only explored Pol α-primase stimulation in vitro and did not investigate in vivo telomeric function or interactions with telomeric DNA (Casteel et al., 2009; Goulian and Heard, 1990). Thus, this work did not address whether CTC1/STN1 promotes general DNA replication or telomere replication. Our results reveal a clear role for CTC1/STN1 in telomere maintenance. However, we cannot rule out additional non-telomeric functions. Indeed, the non-telomeric γH2AX staining after CTC1 knockdown is consistent with a role in DNA replication or repair. One possibility is that CST acts as a specialized replication/repair factor that is needed to reinitiate DNA synthesis by DNA Pol α if a replication block causes uncoupling of polymerase and helicase activity at the replication fork (Heller and Marians, 2006; Yao and O'Donnell, 2009). Such a function might explain the residual exonuclease resistant G-strand signal after CTC1 depletion.

Many of the telomere defects observed after CTC1 depletion can be explained by defects in lagging strand replication either at the chromosome terminus or within the telomeric tract. For example, failure to fill-in the C-strand following telomerase action or C-strand resection would lead to long G-overhangs. Damage to the G-strand might, in turn, result in telomere loss and/or telomere fusions. Likewise, failure to re-initiate lagging strand synthesis after replication fork stalling could lead to loss of large stretches of telomeric DNA and signal free ends.

Given the role played by the *S. cerevisiae* CST complex, one attractive model for CTC1/STN1 function is that it serves to recruit Pol α-primase to the telomeric G-strand after telomerase action and/or C-strand processing. Pol α appears to be recruited to replication forks by Mcm10,

which may in turn interact with the Cdc45/Mcm2-7/GINS replicative helicase (Warren et al., 2008). However, since the G-strand overhang cannot support a conventional replication fork, telomeres appear to require a specialized mechanism to recruit Pol α-primase for C-strand fill-in. Further studies are needed to test this model for CTC1/STN1 function. Additional work will also be required to determine the extent to which the telomeric function of CTC1/STN1 stems from its role in telomere replication versus a more passive function in G-overhang protection. Perhaps the balance between these activities will differ between organisms. For example, the *Arabidopsis* and *S. cerevisiae* complexes may function in both capacities, while the mammalian complex is specialized for telomere replication.

Experimental Procedures

Mutant lines and CTC1 localization

The *ctc1-1* line was identified in the TILLING collection (Till et al., 2003). *ctc1-2* and *ctc1-3* lines were found in the SALK database (stock lines SALK_114032 and SALK_083165, respectively). Genotyping is described in supplemental methods. The *stn1-1* line was previously described (Song et al., 2008). A genetic cross was performed between plants heterozygous for *stn1-1* and for *ctc1-1*. For localization studies, a genomic copy of *CTC1* was cloned into the pB7WGC2 Gateway vector (Karimi et al., 2005). The resulting N-terminal CFP fusion was transformed into wild type *Arabidopsis* (Surovtseva et al., 2007). Cloning, telomere assays and cytology, including FISH, are described in supplemental methods.

Map-based cloning

Map-based cloning was performed essentially as described (Lukowitz et al., 2000). Briefly, a mutant line (*Columbia* ecotype) was out-crossed to wild type *Arabidopsis Landsberg erecta* ecotype. F1 plants were self-propagated to F2. Pools of wild type and mutant plants were generated (~50 plants in each pool) for bulked segregant analysis. CIW5 and CIW6 markers were identified as markers linked to the mutation. 150 individual mutant plants were used to find recombinants in the genomic interval between CIW5 and CIW6. The region containing the mutation was mapped by creating and analyzing new markers. Primer sequences of mapping markers are available upon request.

siRNA-mediated knockdown of HsCTC1

HeLa, MCF7 or 293T cells were subject to two rounds of transfection 24 hrs apart using Lipofectamine2000, Oligofectamine or $CaPO_4$. The final concentration of siRNA duplex (see supplemental methods for sequences) was 50 nM (Ambion) or 100 nM (EZBiolab) for each transfection. The efficiency of CTC1 knockdown was assessed using quantitative real-time RT-PCR with SYBR Green. Regions of *CTC1* and *GAPDH* mRNAs were amplified for each RNA sample. The *GAPDH* mRNA level was used as an endogenous control to normalize the level of *CTC1* mRNA for each sample. The normalized values were plotted relative to the mock-transfected control that was set to 100%. All reactions were performed in duplicate.

Supplementary Material

Refer to Web version on PubMed Central for supplementary material.

Acknowledgments

We thank Fuyuki Ishikawa for communicating results prior to publication. We also thank Jung Ro Lee for two hybrid analysis and Mary Chaiken, Geoffrey Kapler, Rachid Drissi, Erik Hendrickson, Paul Andreasen and Wayne Versaw for helpful comments and gifts of reagents. This work was supported by NIH grants GM065383 to D.E.S., GM041803 and GM73169 to C.M.P., and a Ruth L. Kirschstein National Research Service Award (GM800052) to J.C.L.

References

Armstrong SJ, Franklin FC, Jones GH. Nucleolus-associated telomere clustering and pairing precede meiotic chromosome synapsis in *Arabidopsis* thaliana. J Cell Sci 2001;114:4207–4217. [PubMed: 11739653]

Baumann P, Cech TR. Pot1, the putative telomere end-binding protein in fission yeast and humans. Science 2001;292:1171–1175. [PubMed: 11349150]

Bianchi A, Negrini S, Shore D. Delivery of yeast telomerase to a DNA break depends on the recruitment functions of Cdc13 and Est1. Mol Cell 2004;16:139–146. [PubMed: 15469829]

Bianchi A, Shore D. How telomerase reaches its end: mechanism of telomerase regulation by the telomeric complex. Mol Cell 2008;31:153–165. [PubMed: 18657499]

Casteel DE, Zhuang S, Zheng Y, Perrino FW, Boss GR, Goulian M, Pilz RB. A DNA polymerase-alpha/primase cofactor with homology to replication protein A-32 regulates DNA replication in mammalian cells. J Biol Chem 2009;284:5807–5818. [PubMed: 19119139]

Celli GB, de Lange T. DNA processing is not required for ATM-mediated telomere damage response after TRF2 deletion. Nat Cell Biol 2005;7:712–718. [PubMed: 15968270]

Chandra A, Hughes TR, Nugent CI, Lundblad V. Cdc13 both positively and negatively regulates telomere replication. Genes Dev 2001;15:404–414. [PubMed: 11230149]

Churikov D, Price CM. Pot1 and cell cycle progression cooperate in telomere length regulation. Nat Struct Mol Biol 2008;15:79–84. [PubMed: 18066078]

Churikov D, Wei C, Price CM. Vertebrate POT1 restricts G-overhang length and prevents activation of a telomeric DNA damage checkpoint but is dispensable for overhang protection. Mol Cell Biol 2006;26:6971–6982. [PubMed: 16943437]

Cooper JP, Nimmo ER, Allshire RC, Cech TR. Regulation of telomere length and function by a Myb-domain protein in fission yeast. Nature 1997;385:744–747. [PubMed: 9034194]

de Lange T. T-loops and the origin of telomeres. Nat Rev Mol Cell Biol 2004;5:323–329. [PubMed: 15071557]

Dejardin J, Kingston RE. Purification of proteins associated with specific genomic Loci. Cell 2009;136:175–186. [PubMed: 19135898]

Denchi EL, de Lange T. Protection of telomeres through independent control of ATM and ATR by TRF2 and POT1. Nature 2007;448:1068–1071. [PubMed: 17687332]

Donnelly PM, Bonetta D, Tsukaya J, Dengler RE, Dengler NG. Cell Cycling and Cell Enlargement in Developing Leaves of *Arabidopsis*. Developmental Biology 1999;215:407–419. [PubMed: 10545247]

Fitzgerald MS, Riha K, Gao F, Ren S, McKnight TD, Shippen DE. Disruption of the telomerase catalytic subunit gene from *Arabidopsis* inactivates telomerase and leads to a slow loss of telomeric DNA. Proc Natl Acad Sci U S A 1999;96:14813–14818. [PubMed: 10611295]

Gao H, Cervantes RB, Mandell EK, Otero JH, Lundblad V. RPA-like proteins mediate yeast telomere function. Nat Struct Mol Biol 2007;14:208–214. [PubMed: 17293872]

Garvik B, Carson M, Hartwell L. Single-stranded DNA arising at telomeres in cdc13 mutants may constitute a specific signal for the RAD9 checkpoint. Mol Cell Biol 1995;15:6128–6138. [PubMed: 7565765]

Goulian M, Heard CJ. The mechanism of action of an accessory protein for DNA polymerase alpha/primase. J Biol Chem 1990;265:13231–13239. [PubMed: 2376593]

Grandin N, Damon C, Charbonneau M. Ten1 functions in telomere end protection and length regulation in association with Stn1 and Cdc13. EMBO J 2001;20:1173–1183. [PubMed: 11230140]

Grandin N, Reed SI, Charbonneau M. Stn1, a new Saccharomyces cerevisiae protein, is implicated in telomere size regulation in association with Cdc13. Genes Dev 1997;11:512–527. [PubMed: 9042864]

Grossi S, Puglisi A, Dmitriev PV, Lopes M, Shore D. Pol12, the B subunit of DNA polymerase alpha, functions in both telomere capping and length regulation. Genes Dev 2004;18:992–1006. [PubMed: 15132993]

Guo X, Deng Y, Lin Y, Cosme-Blanco W, Chan S, He H, Yuan G, Brown EJ, Chang S. Dysfunctional telomeres activate an ATM-ATR-dependent DNA damage response to suppress tumorigenesis. EMBO J 2007;26:4709–4719. [PubMed: 17948054]

Gutierrez C. Coupling cell proliferation and developement in plants. Nat Cell Biol 2005;7:535–541. [PubMed: 15928697]

Heacock M, Spangler E, Riha K, Puizina J, Shippen DE. Molecular analysis of telomere fusions in *Arabidopsis*: multiple pathways for chromosome end-joining. EMBO J 2004;23:2304–2313. [PubMed: 15141167]

Heacock ML, Idol RA, Friesner JD, Britt AB, Shippen DE. Telomere dynamics and fusion of critically shortened telomeres in plants lacking DNA ligase IV. Nucleic Acids Res 2007;35:6490–6500. [PubMed: 17897968]

Heller RC, Marians KJ. Replication fork reactivation downstream of a blocked nascent leading strand. Nature 2006;439:557–562. [PubMed: 16452972]

Hockemeyer D, Daniels JP, Takai H, de Lange T. Recent expansion of the telomeric complex in rodents: Two distinct POT1 proteins protect mouse telomeres. Cell 2006;126:63–77. [PubMed: 16839877]

Hockemeyer D, Sfeir AJ, Shay JW, Wright WE, de Lange T. POT1 protects telomeres from a transient DNA damage response and determines how human chromosomes end. EMBO J 2005;24:2667–2678. [PubMed: 15973431]

Hoffelder DR, Luo L, Burke NA, Watkins SC, Gollin SM, Saunders WS. Resolution of anaphase bridges in cancer cells. Chromosoma 2004;112:389–397. [PubMed: 15156327]

Hong JP, Byun MY, Koo DH, An K, Bang JW, Chung IK, An G, Kim WT. Suppression of RICE TELOMERE BINDING PROTEIN 1 results in severe and gradual developmental defects accompanied by genome instability in rice. Plant Cell 2007;19:1770–1781. [PubMed: 17586654]

Iyer S, Chadha AD, McEachern MJ. A mutation in the STN1 gene triggers an alternative lengthening of telomere-like runaway recombinational telomere elongation and rapid deletion in yeast. Mol Cell Biol 2005;25:8064–8073. [PubMed: 16135798]

Karimi M, De Meyer B, Hilson P. Modular cloning in plant cells. Trends Plant Sci 2005;10:103–105. [PubMed: 15749466]

Lei M, Podell ER, Cech TR. Structure of human POT1 bound to telomeric single-stranded DNA provides a model for chromosome end-protection. Nat Struct Mol Biol 2004;11:1223–1229. [PubMed: 15558049]

Lei M, Zaug AJ, Podell ER, Cech TR. Switching human telomerase on and off with hPOT1 protein in vitro. J Biol Chem 2005;280:20449–20456. [PubMed: 15792951]

Li S, Makovets S, Matsuguchi T, Blethrow JD, Shokat KM, Blackburn EH. Cdk1-dependent phosphorylation of Cdc13 coordinates telomere elongation during cell-cycle progression. Cell 2009;136:50–61. [PubMed: 19135888]

Linger BR, Price CM. Conservation of telomere protein complexes:Shuffling through evolution. Crit Rev Biochem Mol Biol. 2009In Press

Lukowitz W, Gillmor CS, Scheible WR. Positional cloning in *Arabidopsis*. Why it feels good to have a genome initiative working for you. Plant Physiol 2000;123:795–805. [PubMed: 10889228]

Lundblad, V. Budding yeast telomeres. Telomeres; de Lange, T.; Lundblad, V.; Blackburn, E., editors. Cold Spring Harbor Laboratory Press; 2006. p. 345-386.

Martin V, Du LL, Rozenzhak S, Russell P. Protection of telomeres by a conserved Stn1-Ten1 complex. Proc Natl Acad Sci U S A 2007;104:14038–14043. [PubMed: 17715303]

Mesner LD, Crawford EL, Hamlin JL. Isolating apparently pure libraries of replication origins from complex genomes. Mol Cell 2006;21:719–726. [PubMed: 16507369]

Mitton-Fry RM, Anderson EM, Hughes TR, Lundblad V, Wuttke DS. Conserved structure for single-stranded telomeric DNA recognition. Science 2002;296:145–147. [PubMed: 11935027]

Miyoshi T, Kanoh J, Saito M, Ishikawa F. Fission yeast Pot1-Tpp1 protects telomeres and regulates telomere length. Science 2008;320:1341–1344. [PubMed: 18535244]

Palm W, de Lange T. How shelterin protects mammalian telomeres. Annu Rev Genet 2008;42:301–334. [PubMed: 18680434]

Petreaca RC, Chiu HC, Eckelhoefer HA, Chuang C, Xu L, Nugent CI. Chromosome end protection plasticity revealed by Stn1p and Ten1p bypass of Cdc13p. Nat Cell Biol 2006;8:748–755. [PubMed: 16767082]

Petreaca RC, Chiu HC, Nugent CI. The role of Stn1p in Saccharomyces cerevisiae telomere capping can be separated from its interaction with Cdc13p. Genetics 2007;177:1459–1474. [PubMed: 17947422]

Puglisi A, Bianchi A, Lemmens L, Damay P, Shore D. Distinct roles for yeast Stn1 in telomere capping and telomerase inhibition. EMBO J 2008;27:2328–2339. [PubMed: 19172739]

Qi H, Zakian VA. The Saccharomyces telomere-binding protein Cdc13p interacts with both the catalytic subunit of DNA polymerase alpha and the telomerase-associated est1 protein. Genes Dev 2000;14:1777–1788. [PubMed: 10898792]

Riha K, McKnight TD, Griffing LR, Shippen DE. Living with genome instability: plant responses to telomere dysfunction. Science 2001;291:1797–1800. [PubMed: 11230697]

Shakirov EV, Shippen DE. Length regulation and dynamics of individual telomere tracts in wild-type *Arabidopsis*. Plant Cell 2004;16:1959–1967. [PubMed: 15258263]

Shakirov EV, Surovtseva YV, Osbun N, Shippen DE. The *Arabidopsis* Pot1 and Pot2 proteins function in telomere length homeostasis and chromosome end protection. Mol Cell Biol 2005;25:7725–7733. [PubMed: 16107718]

Song X, Leehy K, Warrington RT, Lamb JC, Surovtseva YV, Shippen DE. STN1 protects chromosome ends in *Arabidopsis* thaliana. Proc Natl Acad Sci U S A 2008;105:19815–19820. [PubMed: 19064932]

Surovtseva YV, Shakirov EV, Vespa L, Osbun N, Song X, Shippen DE. *Arabidopsis* POT1 associates with the telomerase RNP and is required for telomere maintenance. EMBO J 2007;26:3653–3661. [PubMed: 17627276]

Till BJ, Colbert T, Tompa R, Enns LC, Codomo CA, Johnson JE, Reynolds SH, Henikoff JG, Greene EA, Steine MN, et al. High-throughput TILLING for functional genomics. Methods Mol Biol 2003;236:205–220. [PubMed: 14501067]

Veldman T, Etheridge KT, Counter CM. Loss of hPot1 function leads to telomere instability and a cut-like phenotype. Curr Biol 2004;14:2264–2270. [PubMed: 15620654]

Wang F, Podell ER, Zaug AJ, Yang Y, Baciu P, Cech TR, Lei M. The POT1-TPP1 telomere complex is a telomerase processivity factor. Nature 2007;445:506–510. [PubMed: 17237768]

Wang RC, Smogorzewska A, de Lange T. Homologous recombination generates T-loop-sized deletions at human telomeres. Cell 2004;119:355–368. [PubMed: 15507207]

Warren EM, Vaithiyalingam S, Haworth J, Greer B, Bielinsky AK, Chazin WJ, Eichman BF. Structural basis for DNA binding by replication initiator Mcm10. Structure 2008;16:1892–1901. [PubMed: 19081065]

Wei C, Price M. Protecting the terminus: t-loops and telomere end-binding proteins. Cell Mol Life Sci 2003;60:2283–2294. [PubMed: 14625675]

Wu L, Multani AS, He H, Cosme-Blanco W, Deng Y, Deng JM, Bachilo O, Pathak S, Tahara H, Bailey SM, et al. Pot1 deficiency initiates DNA damage checkpoint activation and aberrant homologous recombination at telomeres. Cell 2006;126:49–62. [PubMed: 16839876]

Xin H, Liu D, Wan M, Safari A, Kim H, Sun W, O'Connor MS, Songyang Z. TPP1 is a homologue of ciliate TEBP-beta and interacts with POT1 to recruit telomerase. Nature 2007;445:559–562. [PubMed: 17237767]

Yang Q, Zheng YL, Harris CC. POT1 and TRF2 cooperate to maintain telomeric integrity. Mol Cell Biol 2005;25:1070–1080. [PubMed: 15657433]

Yao NY, O'Donnell M. Replisome structure and conformational dynamics underlie fork progression past obstacles. Curr Opin Cell Biol. 2009

Ye JZ, Hockemeyer D, Krutchinsky AN, Loayza D, Hooper SM, Chait BT, de Lange T. POT1-interacting protein PIP1: a telomere length regulator that recruits POT1 to the TIN2/TRF1 complex. Genes Dev 2004;18:1649–1654. [PubMed: 15231715]

Zellinger B, Akimcheva S, Puizina J, Schirato M, Riha K. Ku suppresses formation of telomeric circles and alternative telomere lengthening in *Arabidopsis*. Mol Cell 2007;27:163–169. [PubMed: 17612498]

Zellinger B, Riha K. Composition of plant telomeres. Biochim Biophys Acta 2007;1769:399–409. [PubMed: 17383025]

Zubko MK, Lydall D. Linear chromosome maintenance in the absence of essential telomere-capping proteins. Nat Cell Biol 2006;8:734–740. [PubMed: 16767084]

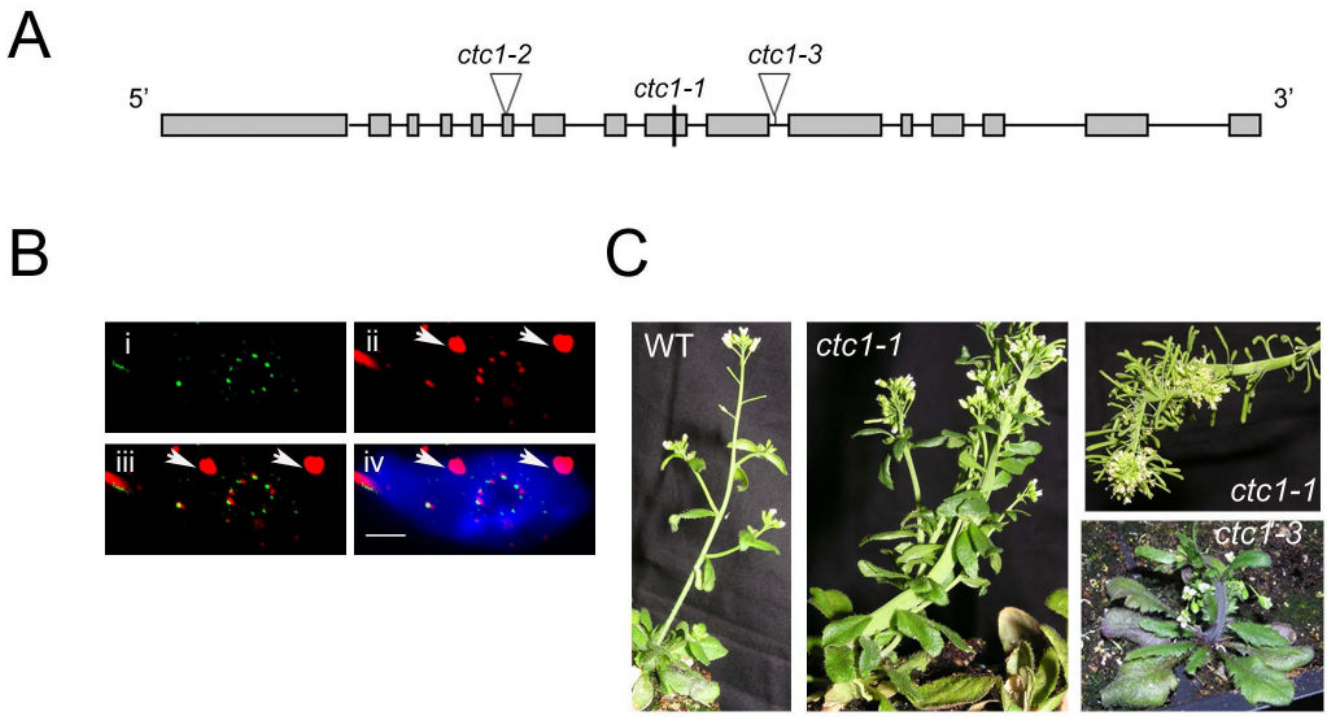

Figure 1.

Identification of CTC1 in *Arabidopsis thaliana*. (A) Top, schematic of the *AtCTC1* gene locus. Rectangles represent exons; horizontal black lines are introns. The positions of the point mutation (*ctc1-1*) and T-DNA insertions (*ctc1-2* and *ctc1-3*) are shown. (B) Co-localization of AtCTC1 and telomeres at the nucleolus periphery of leaf nuclei from seedlings. (i) CFP-AtCTC1 localization detected with anti-GFP antibody; (ii) telomere FISH using probe made from DIG-UTP labeled T_3AG_3-C_3TA_3; (iii) CFP-AtCTC1– telomere merge; (iv) image from panel (iii) is combined with DAPI stained nucleus. The nucleolus appears as a ring where DAPI staining is excluded, arrows in (i)-(iv) indicate internal stretches of telomeric DNA sequence (Armstrong et al., 2001). Scale bar = 2.5 μm. (C) Morphological defects in *ctc1* mutants. Left panel, wild type; middle and right panels, first generation *ctc1-1* and *ctc1-3* mutants of similar age. Fasciated stems and fused organs in *ctc1* mutants are shown. The severity of morphological defects varies among *ctc1* mutants.

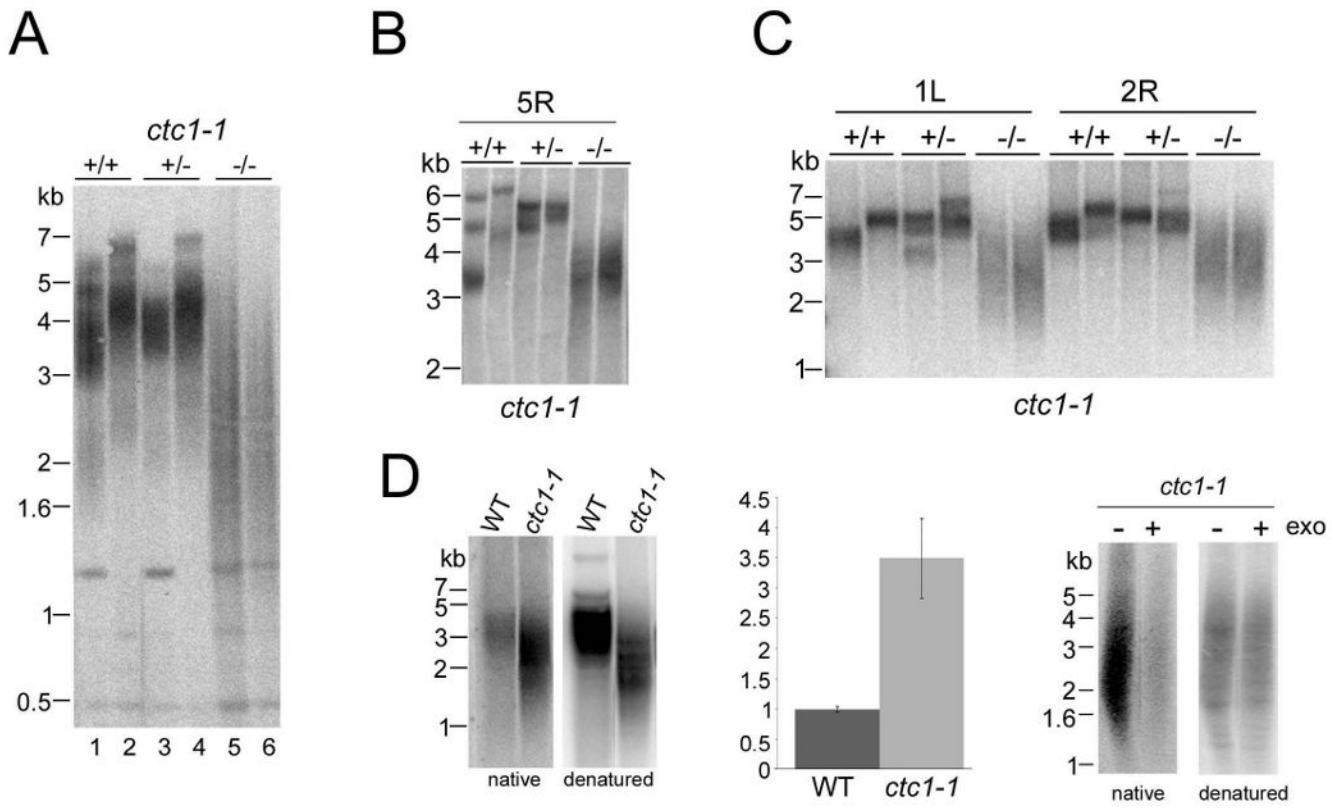

Figure 2.

Telomere length deregulation and increased G-overhangs in *AtCTC1* mutants. (A) TRF analysis of *ctc1-1*. Results are shown for progeny segregated from a parent heterozygous for *ctc1*. (B) Subtelomeric TRF analysis of DNA from *ctc1-1* mutant. DNA blots were hybridized with a probe corresponding to subtelomeric regions on the right arm of chromosome 5 (5R). (C) PETRA analysis of DNA from *ctc1-1* mutants. Results for the 1L and 2R telomeres are shown. (D) In-gel hybridization of $(C_3TA_3)_4$ probe to telomeric restriction fragments under native and denaturing conditions (left). Quantification of *ctc1-1* signal relative to wild type is shown in the middle panel. Data are the average of 8 independent experiments ±SD, (*P*=1.3E-5 Student's t-test). Right panel, in-gel hybridization of *ctc1-1* DNA in the absence (-) or presence (+) of 3′→5′ exonuclease (T4 DNA polymerase). In panels A and C, blots were hybridized with a radiolabeled telomeric DNA probe $(T_3AG_3)_4$. Molecular weight markers are indicated.

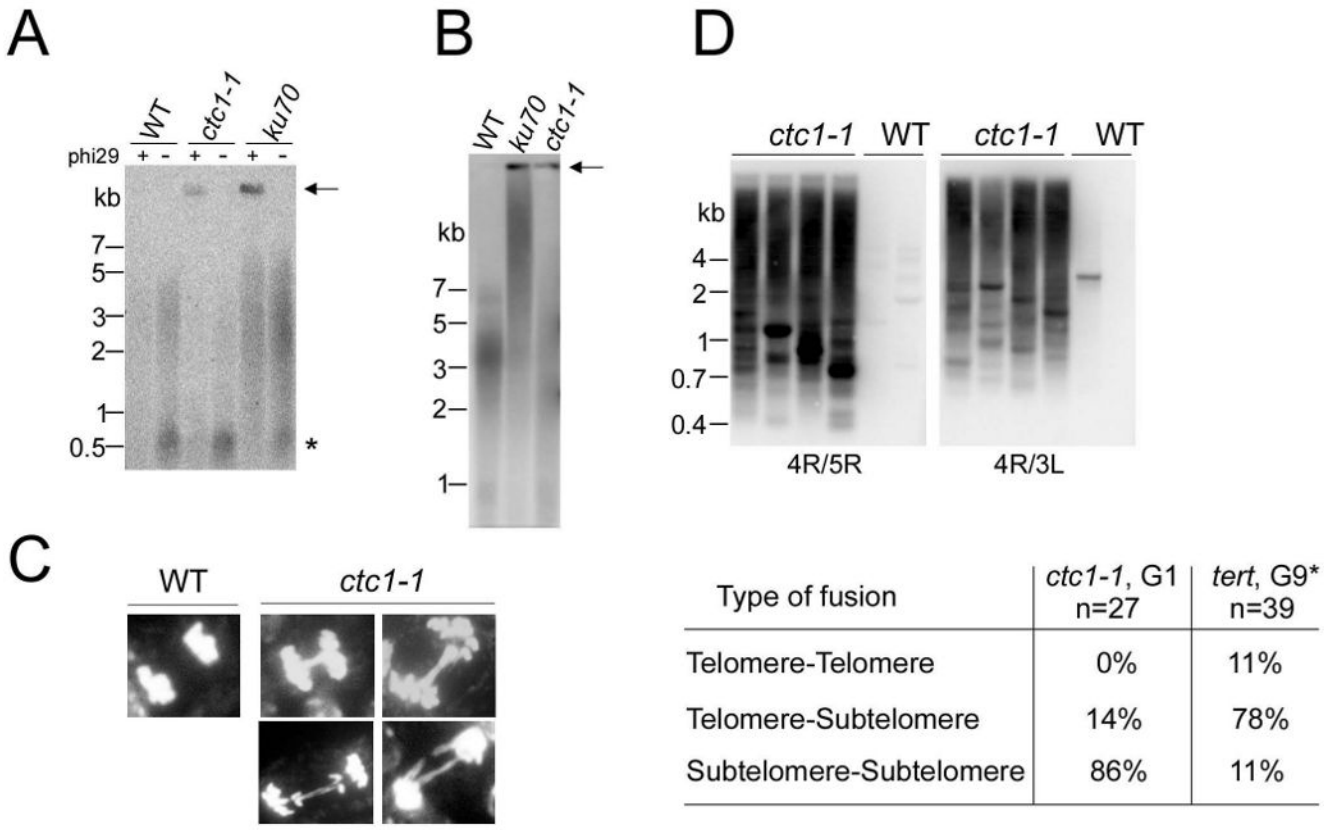

Type of fusion	*ctc1-1*, G1 n=27	*tert*, G9* n=39
Telomere-Telomere	0%	11%
Telomere-Subtelomere	14%	78%
Subtelomere-Subtelomere	86%	11%

Figure 3.

ctc1-1 mutants display elevated telomere recombination and end-to-end fusions. (A) T-circle amplification with *ctc1-1* DNA. Reactions were performed in the presence or absence of phi29 polymerase. *ku70* DNA was used as a positive control. (B) Bubble trapping results for *ctc1-1* and *ku70* mutants. All blots were hybridized with a radiolabeled telomeric probe. In panels A and B, the probe hybridized to both circular and linear telomeric DNA products. Arrows mark TCA product/circles, smears correspond to TRFs and the asterisk indicates an interstitial telomeric repeat signal. (C) Cytogenetic analysis of *ctc1-1* mutants showing DAPI-stained chromosome spreads with anaphase figures. (D) Telomere fusion PCR analysis of *ctc1-1* mutants. Primers were specific for 4R and 5R (left) or 4R and 3L (right). The table shows types of fusion junctions found after sequencing PCR products.

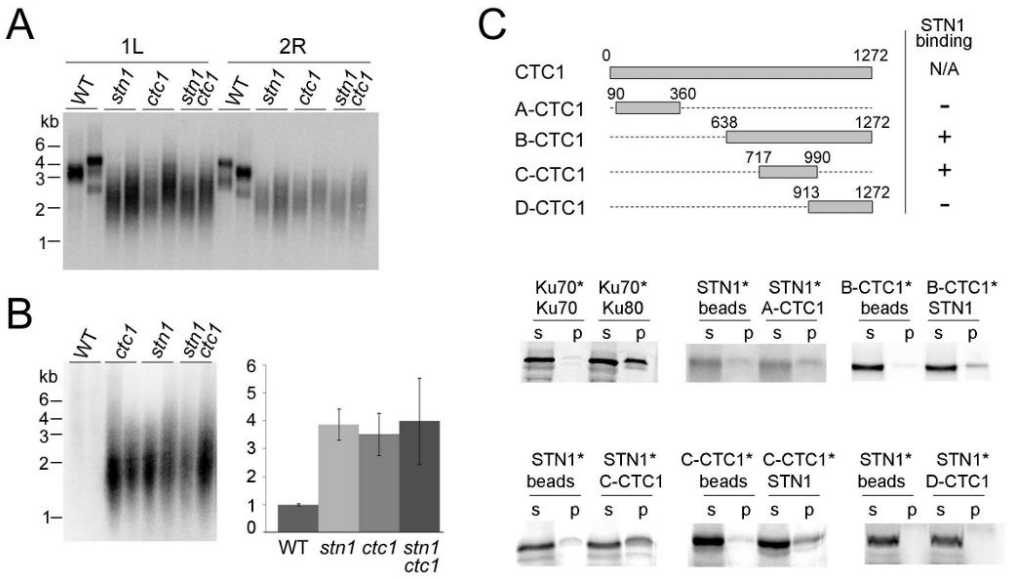

Figure 4.

AtCTC1 and *AtSTN1* function in the same genetic pathway for chromosome end protection and physically interact in vitro. (A) PETRA analysis of telomere length with DNA from *ctc1-1 stn1-1* double mutants, and their *ctc1-1*, *stn1-1* and wild type siblings. (B) G-overhang analysis using in-gel hybridization. Native gel and quantification results (the average of 6 independent experiments ±SD) are shown. $P \leq 0.005$ for all mutant samples compared to wild type, and $P \geq 0.4$ for mutant samples compared to each other. In A and B, all progeny were segregated from a double heterozygous *ctc1-1 stn1-1* parent. Blots were hybridized with a radiolabeled telomeric DNA probe. (C) Top, schematic of the full-length AtCTC1 protein and its truncation derivatives. AtCTC1 fragments that bind AtSTN1 are indicated. Bottom, co-immunoprecipitation experiments conducted with recombinant full length AtSTN1 and truncated AtCTC1 fragments A-D. Asterisks indicate ^{35}S-methionine labeled protein; the unlabeled protein was T7-tagged. S, supernatant; P, pellet. Ku70-Ku80 interaction was the positive control.

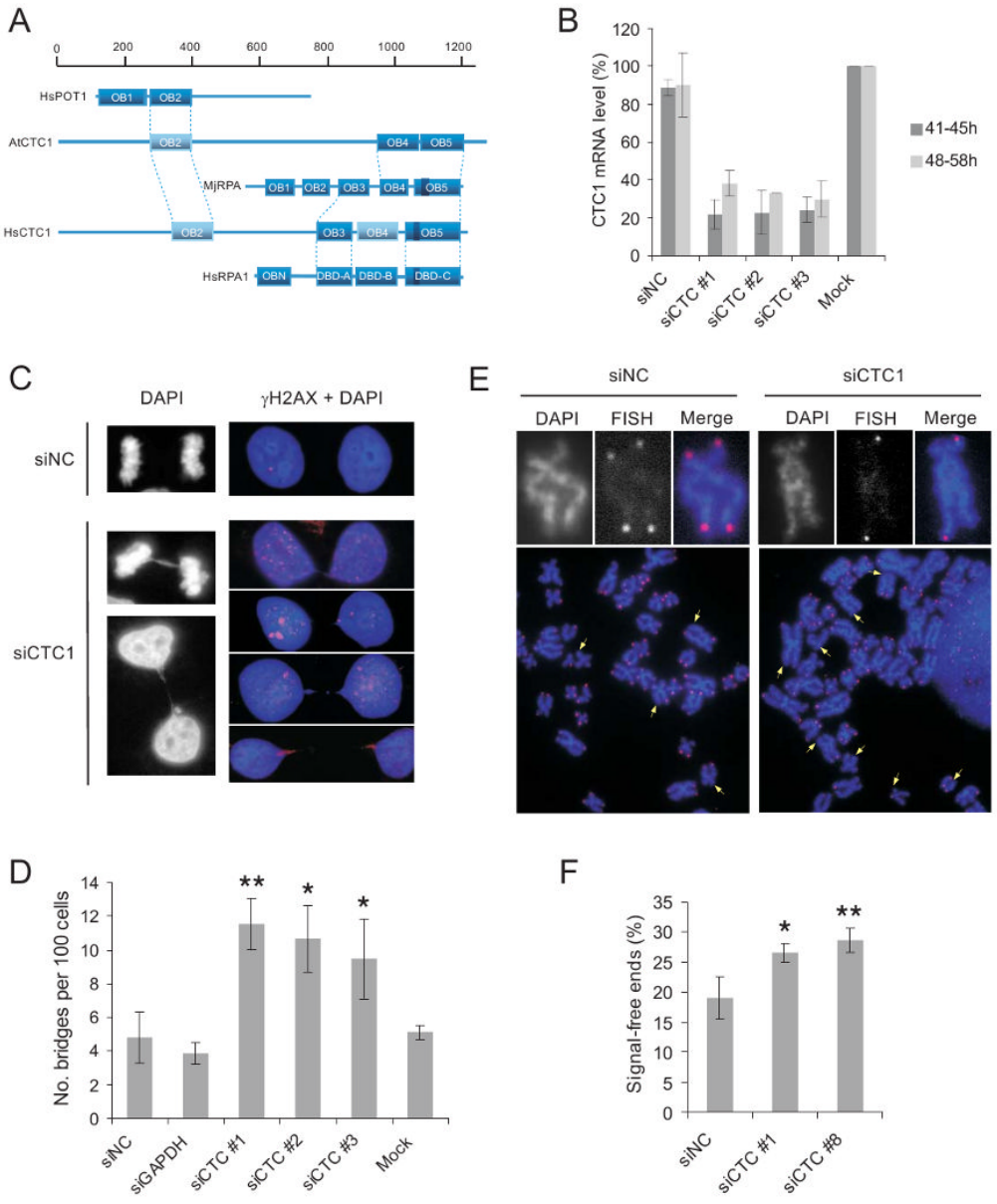

Figure 5.

Depletion of human CTC1 causes genomic instability and sudden telomere loss. (A) Alignment of potential OB-folds in *Arabidopsis* and human CTC1 with OB-fold domains from POT1 and RPA. Dotted lines connect homologous domains. Dark shading, OB-fold homologies predicted by multiple approaches; light shading, homologies predicted by a single method. Dark rectangle within OB5 of HsCTC1 indicates putative Zn finger which is present in human and archaeal RPAs. MjRPA, archeal RPA from *Methanococcus jannaschii*; HsRPA1, human RPA70. (B) Knockdown of CTC1 mRNA in HeLa cells at indicated times after the second transfection. Values are the mean of five independent experiments ± SEM. The percent knockdown is relative to the mock transfection which was set at 100%. NC, non-silencing control; Mock, transfection reagent alone. (C & D) Chromatin bridges and γH2AX staining after CTC1 knockdown in HeLa cells. (C) DAPI staining (blue) shows bridges between interphase cells, γH2AX (red) shows DNA damage foci. (D) Frequency of chromatin bridges.

Mean of three independent experiments ± SEM, stars indicate significance levels (*, $p<0.05$; **, $p<0.01$) from one-tailed Student's t-test. (E & F) Telomere FISH showing signal-free ends 48 hr after CTC1 knockdown in Hela cells. (E) Representative metaphase spreads hybridized with Cy3-OO-$(TTAGGG)_3$ PNA probe. The top panels show magnified view of selected chromosomes. (F) Percent of chromosome ends that lack a telomeric DNA signal after treatment with non-silencing control or CTC1 siRNA. Stars indicate significance of the increase in signal-free ends; significance levels are depicted as in (D).

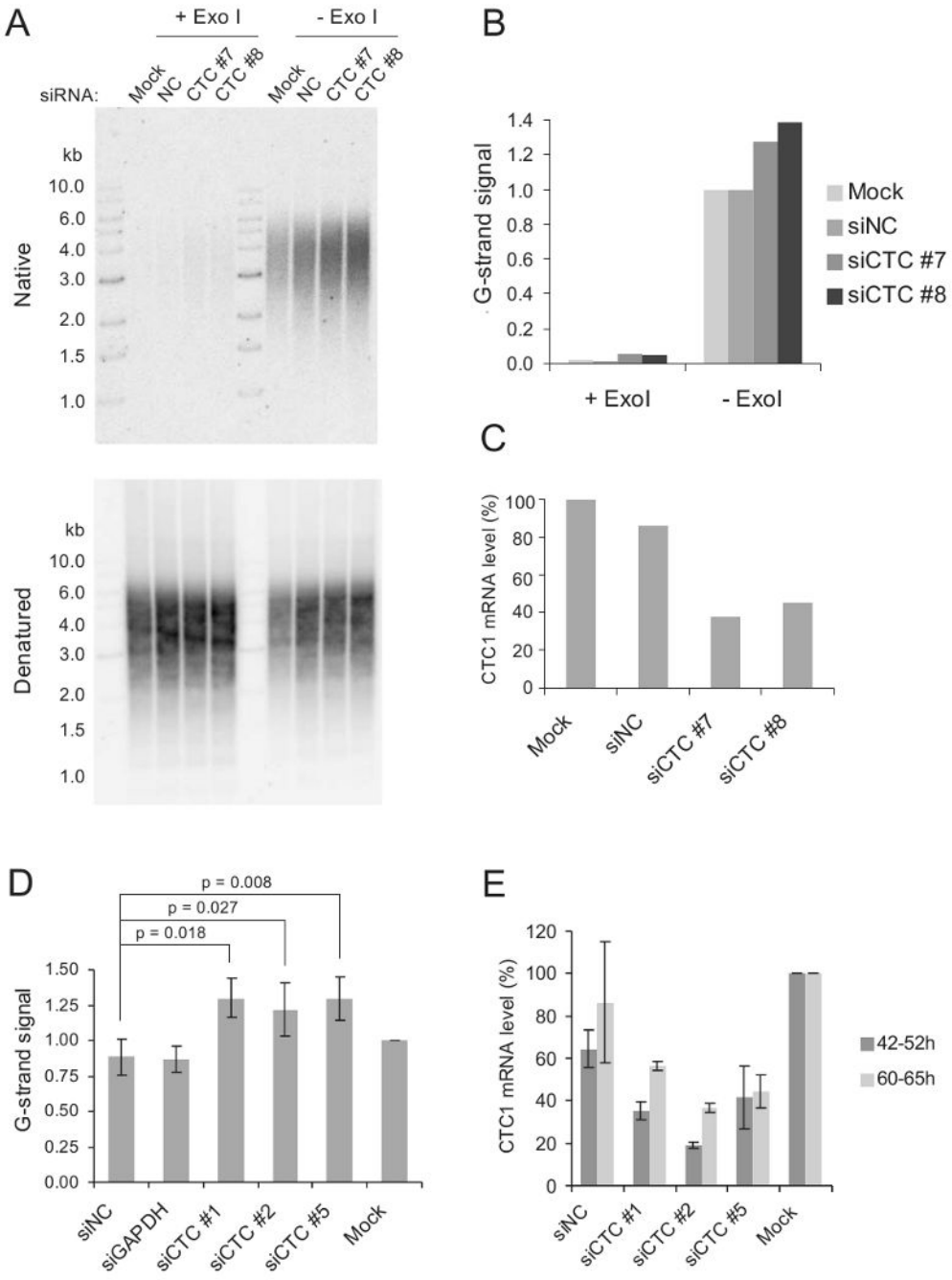

Figure 6.

Deregulation of the G-strand overhang after CTC1-knockdown in MCF7 cells. (A) In-gel hybridization of $(CCCTAA)_4$ probe to telomeric restriction fragments under native (upper panel) or denaturing (lower panel) conditions. +Exo I, DNA samples were treated with Exonuclease I prior to restriction digestion. (B and C) Quantification of G-strand signal (B) or CTC1 mRNA depletion (C) for experiment shown in A. Change in G-strand signal or CTC1 mRNA level is shown relative to the mock transfection. (D) Mean change in G-strand signal after CTC1 knockdown. Data are from three independent experiments ± SEM; p-values are from one-tailed Student's t-test. (E) Mean change in CTC1 mRNA level for experiments shown in (D). See caption to Figure 5B for details.

Table 1

FISH-labeling to identify chromosome ends present in anaphase bridges from *Arabidopsis ctc1-1* mutants.

Chromosome arms	Probe (BAC)	Bridges with signal*	Bridges observed
all but 4S	9 BAC mix	20**	23
1S	F6F3	6	21
1L	F516	5	22
2L	F11L15	3	10
3S	F16M2	5	29
4S	F6N15	6	32
5S	F7J8	7	29
5L	K919	1	8
4S, 2S	25S rDNA	1	7

* Cases where the signal was a doublet are counted as one signal

** All but four signals were doublet